Frontiers in Health Informatics ISSN-Online:2676-7104
www.healthinformaticsjournal.com
2024; Vol 13: Issue 3
Open Access

Optimizing Doxorubicin Efficiency in Breast Cancer Treatment through Chitosan Modified Nanoparticles for Target Drug Delivery

Krishna Champaneria[1], Dr. Prajesh Prajapati[1]
[1]National Forensic Sciences University Gandhinagar, Gujarat.

Cite this paper as: Krishna Champaneria, Prajesh Prajapati (2024) Optimizing Doxorubicin Efficiency in Breast Cancer Treatment through Chitosan Modified Nanoparticles for Target Drug Delivery. *Frontiers in Health Informatics, 13* (3), 8812-8827

Abstract

Background: *The field of biomedical research has been searching for novel platforms for therapeutic and diagnostic uses for a long time. The most recent is the use of nanomaterials, which gave birth to the field of nanomedicine.*

Methodology: *Chitosan/alginate nanoparticles are a unique drug delivery system that target the tumor location by maintaining a pH-dependent drug delivery. Chitosan/alginate is a natural, pH-sensitive, biodegradable, biocompatible, and bioadhesive polymer that is very valuable among other materials. Using a water-in-oil (w/o) emulsion method, alginate/chitosan of varying sizes electrostatically complexes to generate doxorubicin (DOX)-loaded nanoparticles (~80 nm) with remarkable homogeneity and spherical shape. Doxorubicin, an anti-cancer drug, was loaded onto chitosan/alginate nanoparticles and described. The loading of doxorubicin was verified using TEM and FTIR. The murin 4T1 breast cancer cell's viability and cell dead/dead state, as well as drug loading and release properties, were studied.*

Results: *Doxorubicin-loaded nanoparticles' ideal loading efficiency, stability, and release profiles were identified. Following a 72-hour treatment period, cell viability was determined, and the IC50 values for free and encapsulated DOX were 0.13 and 0.15 µg/mL, respectively. While the nanoparticles are quite stable at pH 7.4, the alginate/chitosan NPs discharged the majority of the doxorubicin at pH 5.5.*

Conclusion: *These nanocarriers are a viable platform for the delivery of water soluble medicines because of their good performance, physiochemical features, and ease of manufacture.*

Keywords: *Breast Cancer, Chitosan/Algenate, Doxorubicin, Nanomedicine*,

1. Introduction

In 2020, 10 million fatalities and 20 million new cancer diagnoses were recorded by GLOCAN, with breast cancer accounting for the majority of reported cancer cases [1]. Effectively curing the illness is still a challenge despite current medications, necessitating more specialized and advanced care [2]. Present-day chemotherapy, which uses medications that are poorly soluble in water, has problems with accurate tissue distribution, encourages tumor resistance, is very toxic to normal cells, and causes serious side effects, degradation, poor specificity, and restricted targeting [3, 4]. Therefore, improving medication delivery and development processes represents a critical issue in the fight against cancer [5, 6].

Traditional cancer therapies include radiation, chemotherapy, and/or surgery. Because each of these

approaches has drawbacks of its own, there is a pressing need for novel technologies in the treatment of tumors [7]. The use of nanotechnology becomes more important in the fight against cancer [8]. Finding efficient carriers for therapeutic chemicals is at the heart of using nanotherapy to treat cancer.

The solubility, circulation to cancerous tissues, anti-cancer potency, reduction of inappropriate drug distribution to minimize toxicity in healthy cells, enhancement of drug accumulation at specific sites, bioavailability, and prolongation of drug effectiveness are all enhanced when drugs are encapsulated or entrapped in nanocarriers [9-11]. In chemical approaches to nanomaterials, the idea of nanovehicles is central to the concept of polymer-based NPs as an effective delivery platform because of their small size, large surface area, high drug-loading capacity, ease of surface customization, and increased stability of nanoparticle formulations [12,13].

Natural polymers with mucoadhesive, biodegradable, and biocompatible qualities, such as chitosan and alginate, are used in pharmaceutical and biomedical applications for drug delivery and cell encapsulation [14]. Water-soluble sodium alginate is a salt that is obtained from alginic acid, which is present in brown algae species. It is widely used in the food, beverage, bioengineering, and pharmaceutical sectors [15].

When sodium alginate is soluble, it may undergo cross-linking that is aided by divalent cations such as Mg^{2+} and Ca^{2+}. This results in the formation of what are known as "egg box junctions," which ultimately produce insoluble calcium alginate [16]. Conversely, the biopolymer chitosan is derived from the polysaccharide chitin via a process known as deacetylation, which is usually not fully completed. Chitosan has a pKa of around 6.5. Its amino groups may be protonated in slightly acidic conditions, which gives the glucosamine residue a positive charge. Compared to chitin, chitosan has different physical and chemical characteristics because of these positive charges. Chitosan has a wide range of uses because of its good film-forming ability, affordability, biocompatibility, non-toxicity, inertness under physiological conditions, antibacterial properties, strong mechanical strength, and chemical modification susceptibility [17, 18].

Chitosan's positive charges have made it easier to utilize in a variety of applications, such as materials for treating wounds [19], enhancers for absorption through intestinal epithelium, and mucosal sites for proteins, peptides, and medications [20]. Additionally, it has been used to boost plant growth and support plant defenses against fungal diseases. Furthermore, it has been shown that chitosan is useful for immobilizing cells and enzymes [21]. The enhanced activity of alginate and chitosan in nanoparticle form, which is ascribed to their tiny size and the quantum size effect, makes them favored in many applications [22].

Numerous synthetic approaches, including layer-by-layer procedures [23], emulsification [24], and nanoprecipitation [25], may be used to generate polymer nanocarriers [26]. The final nanocarrier's shape, morphology, integration, and ability to encapsulate therapeutic drugs are greatly influenced by the synthesis method that was selected [26]. Complexes of alginate and chitosan have been widely used to manufacture a variety of medicinal payloads. Examples include esculin for the treatment of nephrolithiasis [27], insulin for protein delivery [28], temoporfin for photodynamic therapy [29], gatifloxacin for ocular administration [30], and chemotherapeutic drugs like doxorubicin (DOX) and paclitaxel for the treatment of lung cancer [31]. The particular emphasis of this study is on doxorubicin (DOX), a chemotherapeutic drug sold under the brand name Adriamycin that is produced from a type of bacteria. Here, DOX—which is renowned for its inherent fluorescence—is used as a prototype medicinal substance.

In cancer treatment, DOX works by intercalating with DNA to limit the production of macromolecules [32, 33]. It is widely used to treat a wide range of tumors, such as soft tissue sarcomas, carcinomas, and hematological malignancies [34]. Its lack of tumor cell selectivity, however, limits its therapeutic utility [35] by producing serious adverse effects such cardiotoxicity, anaphylaxis, and disturbances in intracellular biochemical pathways [36, 37]. In tumor cells, DOX has a poor mitochondrial damage pathway despite its quick entrance into the nucleus of the cell [38, 39]. By using engineered nanocarriers, more especially chitosan-modified nanoparticles, to increase DOX's anticancer efficacy via targeted drug delivery systems, the current work seeks to solve the shortcomings of DOX in cancer treatment [40, 41].

2. Methodology:

The following sources provided the resources utilized in the study: The following materials were purchased from Sigma-Aldrich (St. Louis, MO): dodecylamine (98%), chitosan (50,000–190,000 molecular weight range with a deacetylation level of 75–85%), and sodium alginate (12,000–40,000 molecular weight range). All materials were used exactly as supplied. The source of doxorubicin hydrochloride was MedChem Express (Monmouth, NJ). The suppliers of cyclohexane and hydrochloric acid were Fisher Scientific (Fair Lawn, NJ). The alginate, chitosan, and doxorubicin hydrochloride were dissolved in an 18 MΩ Milli-Q water source before being added to the mixture.

2.1 Nanoparticle Formulation

A glass scintillation vial containing 50 mg of sodium alginate powder was filled with 4 mL of Milli-Q water and allowed to dissolve. To accomplish dissolution, moderate mixing was carried out on a stir plate for thirty minutes using a stir bar. One scintillation vial was filled with 60 mg of chitosan powder, 3 mL of Milli-Q water, and 1 mL of 1 M HCl. To help the chitosan dissolve, this mixture was agitated for 30 minutes on a stir plate with a stir bar (an acidic atmosphere is important for this procedure). A 50 mg/mL aliquot of doxorubicin hydrochloride was obtained, and 10 mL of Milli-Q water was used to thoroughly dissolve it. The concentrations of the produced stock solutions were 5 mg/mL for doxorubicin, 20 mg/mL for chitosan, and 15 mg/mL for alginate. 100 mL of cyclohexane was put in a fume hood to a 100 mL PYREX reusable media storage container. Dodecylamine was melted by slowly heating it under warm tap water for one minute, even though it was a solid at room temperature. Next, 2 milliliters of the liquid dodecylamine were pipetted into the 100 milliliters of cyclohexane, which is now regarded as the solid phase. This bottle was put on a 1000 rpm stir plate. Following that, 100 microliters of the 15 milligram per milliliter alginate solution were pipetted straight into the organic phase and stirred for a duration of 15 minutes. A chitosan and "loading" material solution was made while the alginate was blending in the organic phase. To achieve therapeutic loading, a mixture of 20 µL of the 5 mg/mL DOX solution and 80 µL of the 20 mg/mL chitosan solution was used. Then, after the 15 minutes of alginate mixing, 100 µL of this mixture was introduced to the organic phase. When the chitosan mixture was added to the organic phase, a shift in turbidity was seen. Instead of adding the 5 mg/mL doxorubicin solution to the 80 µL of chitosan solution, 20 µL of Milli-Q water was added in order to create empty nanoparticles. After making this modification, the chitosan mixture was added to the organic phase and stirred for 15 minutes.

2.2. Nanoparticle Characterization

- **Size and zeta potential**

The Malvern Zetasizer ZSP (Malvern Instruments, UK) was used to characterize size and zeta potential. The

numbers given are the mean ± standard deviation of the three measurements, which were done in triplicate.

- **Transmission Electron Microscopy (TEM).**

To get further insight into the shape of the nanoparticles and to validate size measurements, transmission electron microscopy (TEM) was used. A Technai F-20 transmission electron microscope running at 4200 eV was used to capture TEM pictures. Ten microliters of post-filtered nanoparticle solution were dropwise deposited onto the copper surface of the formavar/carbon backed TEM grid (Ted Pella) in order to prepare the TEM grids. To guarantee adequate drying, wet TEM grids were covered and left in a desiccator for the whole night before imaging.

It was not modified or coated in any way before being allowed to dry at ambient temperature and then analyzed using a TEM. From measured particles visible by TEM images, mean diameters and size distribution of diameters were collected and analyzed using the SPSS 11.0 software file.

- **FTIR analysis**

To analyze the molecular structure of the alginate and chitosan nanoparticles, Fourier-transform infrared (FTIR) absorption spectra of each sample were obtained. With a Jasco 460 Plus spectrophotometer from the USA, the 400–4,000 cm-1 range was used for this. Room-temperature KBr pellets were used to prepare the samples for analysis.

32 scans were collected for every sample, guaranteeing a thorough procedure of data acquisition. The effective resolution of the spectrophotometer was adjusted to 4 cm-1. The goal of this process was to get comprehensive infrared absorption spectra, which would allow for the analysis and recognition of distinctive functional groups and chemical bonds found in chitosan and the resultant alginate nanoparticles.

2.3 DOX concentration evaluation

Using the fluorescence that the nanoparticle solution naturally has, the concentration of DOX in the solution was ascertained by contrasting the fluorescence of the DOX-containing nanoparticle solution with a standard curve of the drug solutions. 470/550 nm fluorescence was measured using a Tecan M200 Infinite plate reader. This procedure assisted in determining the amount of DOX contained in the nanoparticle solution. By comparing the amount of DOX found in the final nanoparticle solution to the amount of DOX added originally during the synthesis, encapsulation efficiency was determined. The purified nanoparticle solution was sectioned into 100 µL aliquots and put in Slide-A-Lyzer MINI dialysis machines with a molecular weight cutoff of 2 kDa in order to determine the drug release kinetics from the nanoparticle solution over time. These gadgets were gently shaken while immersed in 20 mL quantities of PBS. The quantity of DOX released was measured using fluorescence on the retentate samples at different times. To understand the drug release profile, many time points (1, 3, 5, 9, 24, 48, and 72 hours) were assessed in duplicate after the first measurement.

ThermoFisher's Nicolet iS5 Infrared Spectrophotometer was used for the infrared spectroscopy study. To measure total internal reflectance, dry samples were compressed and positioned over the diamond filament. High resolution spectra were obtained for alginate, chitosan, DOX, and lyophilized nanoparticles in the wavelength range of 4000 to 400 cm−1. The purpose of this investigation was to provide light on the component species that make up the final nanoparticle structure.

2.4. Cell culture

The 4T1 murine breast cancer cells, obtained from Waltham, Massachusetts-based PerkinElmer, were cultured in RPMI 1640 media that was enhanced with 1% penicillin/streptomycin and 10% fetal bovine serum (FBS). Before being used in viability tests, the cells were passaged through and divided at least twice after being grown to a confluency of around 90%.

In a Corning 96-well plate with transparent bottom and black walls, the cells were counted and diluted to obtain a seeding density of 2000 cells per well before plating. A ThermoFisher Countess II FL Automated Cell Counter was used to count the concentrated cell suspension prior to plating. Using an INTEGRA ASSIST automated pipetting robot from Integra, diluted cell suspensions were pipetted into each well at a volume of 100 µL, using a typical pipetting/mixing methodology. The next day, the cells were dosed after they had stabilized over night.

The nanoparticle and/or free medication solutions were sterilely filtered through a 0.20 µm filter on the days of dosing. To produce media solutions containing the nanoparticles and/or free drug solutions, a dosing plate was created under sterile circumstances. 10% DMSO was added to the positive cell kill control wells, whereas the RPMI medium was used in the untreated wells. In order to reduce evaporation-related irregularities, the plate's exterior wells were kept unoccupied.

Each well's growth medium was aspirated, and the wells were dosed appropriately. Half-fold dilutions of one produced nanoparticle solution were applied to columns 2–9, rows B–D. Half-fold dilutions of either empty nanoparticle solutions or free doxorubicin were administered to columns 2–9, rows E–G. Columns 10–11, rows B–D received the positive control, whereas columns 10–11, rows E–G received the negative control. For the purpose of maintaining constant liquid levels across the plate, phosphate-buffered saline, or PBS, was pipetted into the diamond gaps between the wells. The intended assay timepoint was then reached by incubating the plate.

2.5. Cell Viability Assay

72 hours after dosing, the wells' media was aspirated, cleaned three times with PBS, and replaced with fresh media containing two drops per milliliter of media. Each well received an addition of ThermoFisher's NucBlue live cell reagent and NucGreen dead cell reagent. Before the cells were fixed with formalin, they were given 30 minutes to incubate with the reagents and three additional PBS washes. After giving the cells 30 minutes to fix in the formalin, they underwent three additional PBS washes. The cells were photographed using the DAPI and GFP filter sets on an EVOS FL Auto Imaging System (ThermoFisher) with a 20X objective after 100 µL of PBS was added to each well.

2.6. Data analysis

The gathered data were shown as the means ± standard deviation from a minimum of three different experiments. The Student's t-test was used to evaluate the variations in the group means; statistical significance was defined as $*P < 0.05$, $**P < 0.01$ or $***P < 0.001$.

3. Results and discussion

The procedure that produced and characterized the alginate-chitosan nanoparticles with DOX included an interaction between the positive amine groups on chitosan polymers and the negative carboxylic acid groups on alginate strands. This contact served as the starting point for the complexation that produced the nanoparticles, which happened in an organic solution that functioned as the distributed aqueous phase.

The aqueous phase included water, alginate, and chitosan, whereas the organic phase contained cyclohexane and dodecylamine. The nanoparticles went through two stages of filtering after the creation and extraction

process: a low-pass 100 kDa filter was used to remove bigger aggregates, and a high-pass 10 kDa filter was used to remove smaller contaminants. Before being used in in vitro tests, the particles were cleaned by washing them and then passing them through a 0.20 μm syringe filter to guarantee sterility.

3.1. FTIR analysis

The efficacy of the nanoparticle preparation process was examined in terms of chemical structure using FTIR analysis. Figure 1 displays the FTIR spectra of chitosan, sodium alginate, and the produced nanoparticles of chitosan and alginate. The typical sodium alginate peaks (Fig. 2a) are 1,617 cm-1 for COO–(asymmetric stretching), 3,397 cm-1 for O–H stretching, 1,028 cm-1 for C–O–C stretching, and 1,429 cm-1 for COO–(symmetric stretching) [42]. The cross-linking of sodium alginate with Ca2+ results in a clear shift to lower wavenumbers and a reduction in the strength of the COO– stretching peak. Moreover, the sodium alginate's C-O-C stretching peak has been moved to a lower wavenumber, where its strength is decreased. This suggests the existence of partial covalent interaction between the calcium atoms and the oxygen atoms of the ether groups as well as ionic bonding between the calcium ions and the carboxyl groups of sodium alginate [43].
The N–H, amide I, and amide III groups contained in chitosan are responsible for three distinct absorption bands at 3,413, 1,672, and 1,423 cm-1, as shown in Fig. 2c [43]. These distinctive absorption bands are also visible in the FTIR spectra of the produced chitosan nanoparticles, as shown in Fig. 2d. Additionally, the produced chitosan nanoparticles' FTIR spectra do not display any extra absorption peaks, indicating that the nanoparticles' chemical structure remained unchanged throughout preparation. Fig. 1 shows the loaded alginate and chitosan nanoparticle product together with doxorubicin. In the spectra, there are several overlapping peaks from 1000 to 1800 cm−1, which are probably the carboxylic acid peaks from alginate and peaks supplied by the primary amines from chitosan. This might indicate that both alginate and chitosan were present in the nanoparticle product. The large peak at around 3600 cm−1 is probably caused by the water that is remaining in the lyophilized nanoparticle product. Since that peak is only present on the chitosan, the little peak adjacent to it may be caused by the amines from the chitosan.

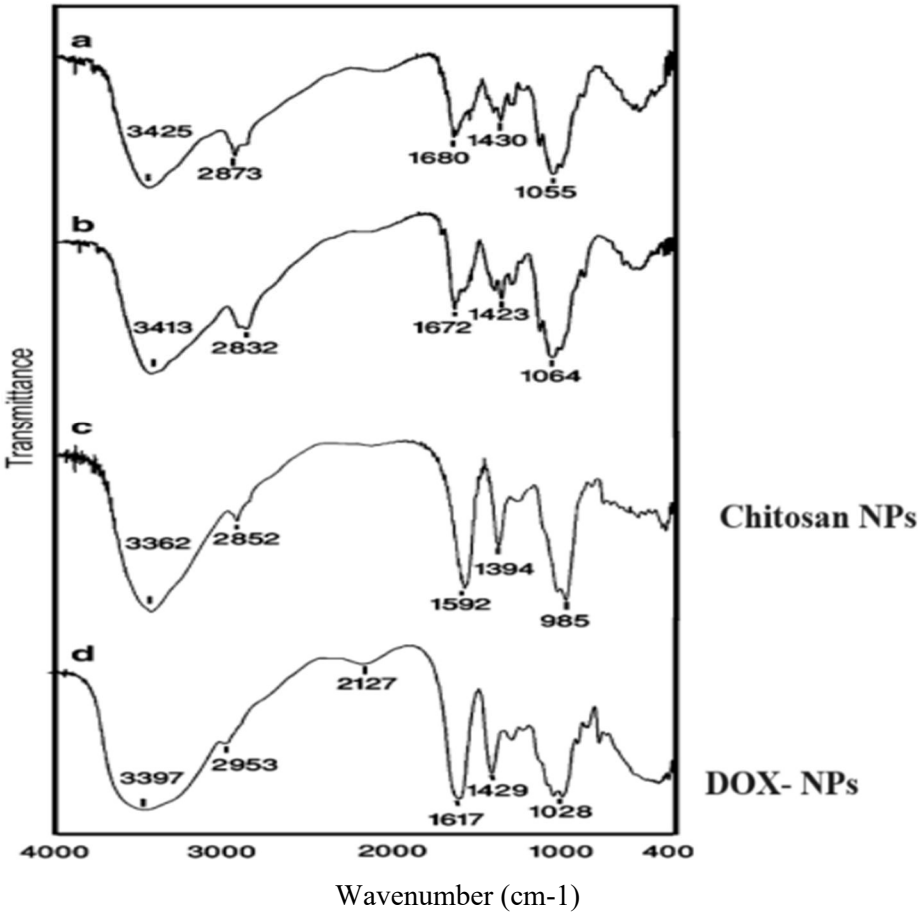

Fig. 1: FTIR spectra of a) alginate, b) alginate nanoparticles, c) chitosan, d) chitosan nanoparticles

3.2. Size distribution

Fig. 2A shows the size distribution of the nanoparticles, with an average size of 90.2± 3.7 nm. Furthermore, the presence of carboxylic acids on the alginate chains was shown to be responsible for the negative surface charge indicated by the zeta potential, which was found to be −26.5 ± 1.4 mV. A transmission electron microscopy in Figure 2B attests to the nanoparticles' spherical shape and size. It's important to remember that earlier research by Kuboi et al. [44] and Kiyoyama et al. [45] has emphasized the role reversing micelle size plays in regulating chitosan and alginate nanoparticle dimensions.

3.3. TEM analysis

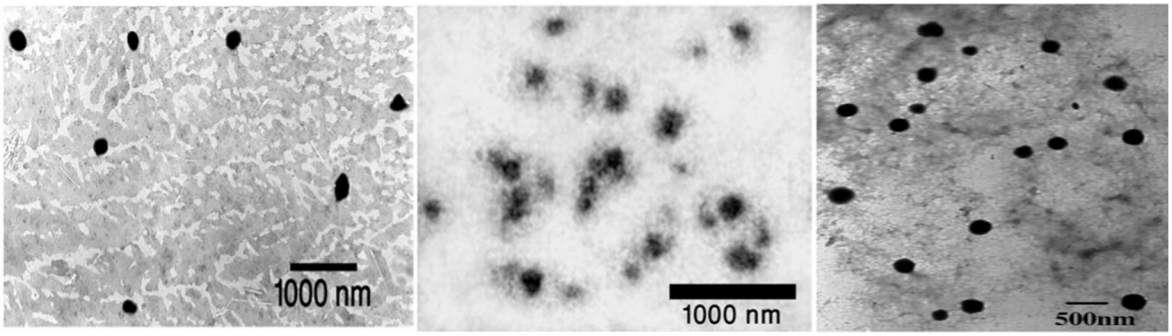

(a) **(b)** **(c)**

Fig. 2: TEM micrographs and diameter distributions of a) alginate nanoparticles, and b) chitosan nanoparticles c) DOX loaded alginate/chitosan nanoparticles

Figures 2a, b, and c, respectively, show the TEM micrograph and the size distribution of the alginate and chitisan nanoparticle and DOX loaded nanoparticle samples. The almost spherical shape of the alginate nanoparticles is seen in the picture. Conversely, chitosan nanoparticles do not seem to be perfectly spherical in form. The electrostatic repulsion between cationic CTAB and cationic chitosan in a water pool, which produces weak and imperfectly chitosan reverse micelles, is the cause of this discrepancy.

Using a W/O microemulsion mostly constituted of cyclehexane as the solvent, n-hexanol as a co-solvent, and Triton X-100 as the surfactant, several researchers [46-48] have created chitosan nanoparticles. According to the work of Jiang and coworkers [49], the size of chitosan nanoparticles was stated to be smaller in these works than it was in our investigation.

3.4. Drug release

A dialysis-based technique was used to assess DOX release from the alginate-chitosan nanocarriers. The nanoparticle solution was dialyzed against 20 mL of pH 7.4 PBS after being split into 21 aliquots, each containing 100 µL. Three samples were taken at different times (1, 3, 5, 9, 24, 48, and 72 hours), and their fluorescence was compared to a doxorubicin standard curve. Figure 3 shows the lost DOX relative to the original quantity at each time point. An encapsulation effectiveness of 8.3% was shown by the first fluorescence measurements, which showed a concentration of around 8.3 µg/mL (0.1 mg DOX added into the system). Within the first 24 hours, there was a notable release of DOX, with around 20% of the medication remaining in the body at that time. By the nine-hour point, around 60% of the DOX was still in the nanoparticle solution at physiological pH, showing a steady release pattern throughout the course of the experiment. This shows that doxorubicin displayed controlled release instead of a sudden burst at normal pH values, mimicking the length of time it would be delivered in vivo.

On the other hand, at pH 5.5, around 70% of the DOX was released by the 8-hour mark, and by the 24th hour, 90% of the DOX had been released. This quick release at an acidic pH shows that the particles release the medication more easily in these conditions. This rapid release, while not originally planned, is in line with the objective of optimizing treatment efficacy in moderately acidic environments, such as the tumor microenvironment (~pH 6.7) or endosomes (pH 5–6) [50, 51].

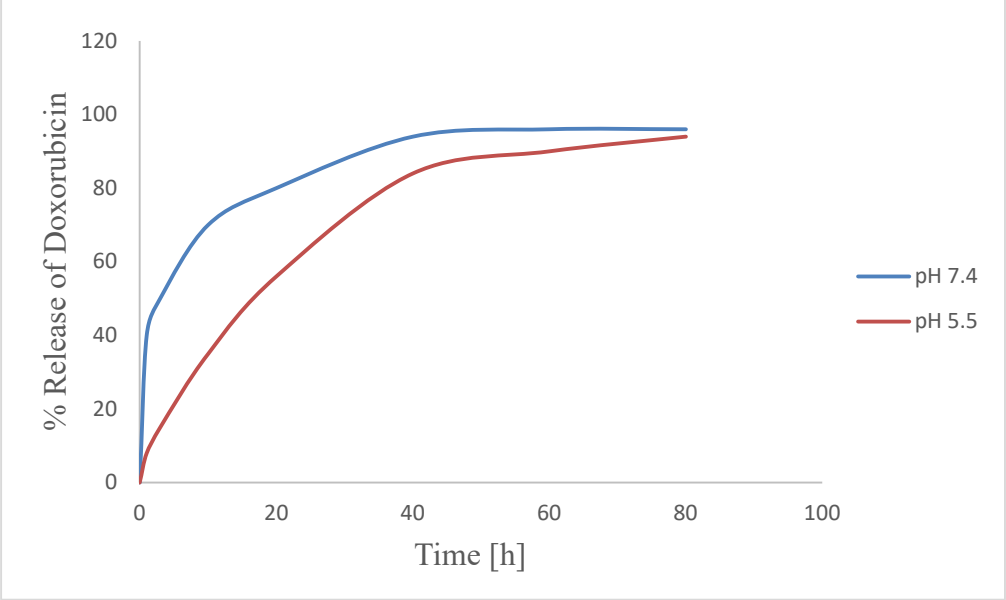

Fig. 3. Release curves for alginate-chitosan nanoparticles in different environments.

3.5. Cell Uptake and Toxicity

The absorption of alginate-chitosan nanoparticles by 4T1 murine breast cancer cells is shown in Fig. 4 after a 72-hour period. The cells in the top two photos (left to right) are treated with empty alginate/chitosan nanoparticles and untreated cells. Cells treated with DOX (left) and alginate-chitosan nanoparticles containing DOX (right) are shown in the bottom photographs (left to right). The intrinsic DOX, which was found using a green fluorescent protein filter set, appears in red close to the nucleus' periphery after fixation, whereas DAPI staining in blue emphasizes the cell nuclei. When compared to the untreated well, the addition of DOX limits cell proliferation, demonstrating its inhibitory impact on 4T1 cell growth. Because there is no DOX in those wells, the red channel is empty in both the untreated sample and the sample treated with empty nanoparticles. Whether unencapsulated or encapsulated, the green signal of DOX, which colocalized with the nucleus in both DOX-containing samples, shows the successful entrance of DOX into the cells. The drug's effectiveness depends on this cellular absorption, which is consistent with a number of previously outlined processes.

The initial lower concentration of DOX in the nanoparticles compared to the beginning concentration utilized for the dose-response curve is the reason for the divergence in concentrations, even though they are not quite equal (0.20 μg/mL for encapsulated vs. 0.17 μg/mL for free DOX). The encapsulated version has potential for in vivo translation because of its regulated release of DOX and increased probability of reaching the tumor environment, as well as its controlled release at physiological pH and longer circulation duration.

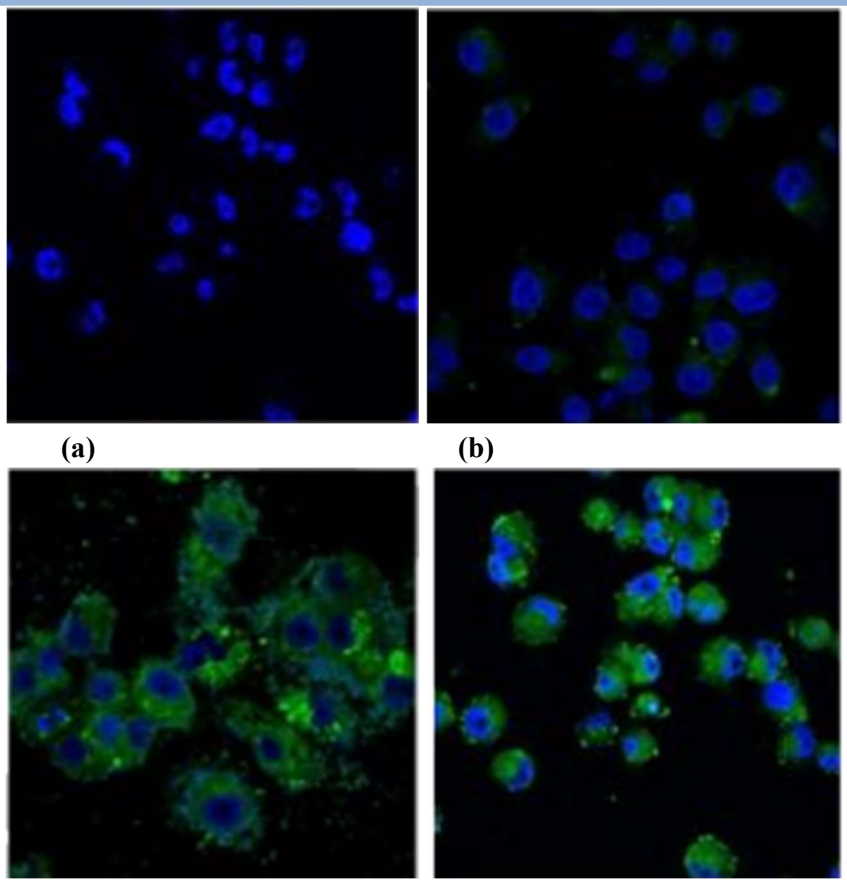

Fig. 4. Fluorescence images showing DOX uptake after 72 h exposure in 4 T1 cells. Treatments are: (a) No treatment, (b) 0.20 µg/mL (DOX equivalent nanoparticle number) empty alginate-chitosan nanoparticle treatment, (c) 0.17 µg/mL free DOX, (d) 0.20 µg/mL DOX-loaded alginate-chitosan nanoparticles. Blue indicates cell nuclei; green indicates presence of DOX.

Several treatments, including empty nanoparticles, free DOX, and alginate/chitosan nanoparticles containing encapsulated DOX, were given to the cells in order to assess the effectiveness of alginate-chitosan nanoparticles against the 4T1 cancer cell line. The Alamar Blue reagent was used to measure the cell survival after a 72-hour exposure to various treatments. After 72 hours, the percentage of cells that remained viable after being exposed to varying quantities of free DOX and alginate-chitosan nanoparticles containing DOX is shown in Fig. 5a, which also shows the DOX concentration in each scenario. For free DOX and encapsulated DOX, the IC50 values that were obtained were 0.13 and 0.15 µg/mL, respectively. Interestingly, the IC50 value of free DOX against 4T1 cells after 72 hours is in good agreement with the results reported by Du et al. [52]. Both the free and encapsulated drug's dose-response curves and matching IC50 values show similarities, suggesting a similar therapeutic effect. If the carrier is not intrinsically hazardous, the encapsulated treatment should theoretically exhibit comparable or somewhat higher IC50 values as a result of the drug's regulated release.

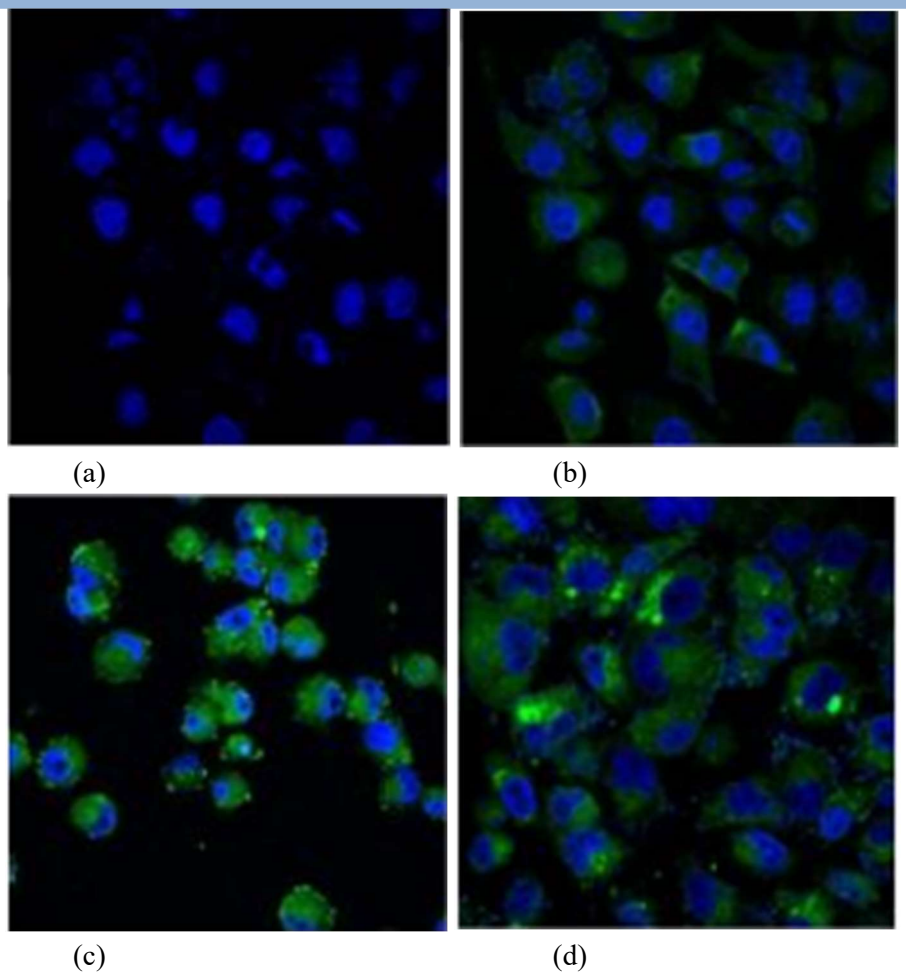

Fig. 6. Fluorescent images of LIVE/DEAD assay. Blue indicates all cell nuclei; green indicates dead cells. Treatments are: (a) No treatment, (b) 0.20 µg/mL (DOX equivalent nanoparticle number) empty alginate-chitosan nanoparticle treatment, (c) 0.17 µg/mL free DOX, (d) 0.20 µg/mL DOX-loaded alginate chitosan nanoparticles. Lower number of cells in DOX treatment images due to presence of therapeutic inhibiting cell proliferation.

Finding the dose-response relationship for the empty alginate/chitosan carrier was a crucial step in the examination of the carrier's toxicity, as shown in Fig. 5b. Based on the available evidence, it seems that the unloaded nanoparticles have low toxicity and are not expected to result in considerable cell death. Duplicate plates that were treated exactly like the viability plates had their cell viability evaluated using a LIVE/DEAD cell test in order to examine cell death in more detail. In this experiment, dead cells show a green signal that overlaps with the nuclei, whereas all nuclei are labeled blue. Figure 6 shows the results of the assay:

There are not many dead cells in these wells, as seen by the (a) empty nanoparticle photos and (b) no treatment images that show a few cells with a green signal. Multiple cells with a strong green signal around their nuclei are seen in (c) cells treated with DOX and (d) alginate/chitosan nanoparticles treated with DOX, indicating a significant number of dead cells. Because DOX inhibits the proliferation of cells inside the well, these wells have fewer cells overall.

The LIVE/DEAD assay's qualitative toxicity evaluation combined with the Alamar Blue assay's quantitative analysis shows how effective DOX is in killing 4T1 cells. On the other hand, Dönmez's 2010 work showed

that both sensitive and doxorubicin-resistant MCF7 cells may efficiently internalize CS MNPs (Chitosan Magnetic Nanoparticles) loaded with the drug. Because P-glycoprotein (P-gp) is highly expressed on the cell membrane of drug-resistant MCF-7 cells, doxorubicin normally does not accumulate efficiently in the cytoplasm of these cells [53].

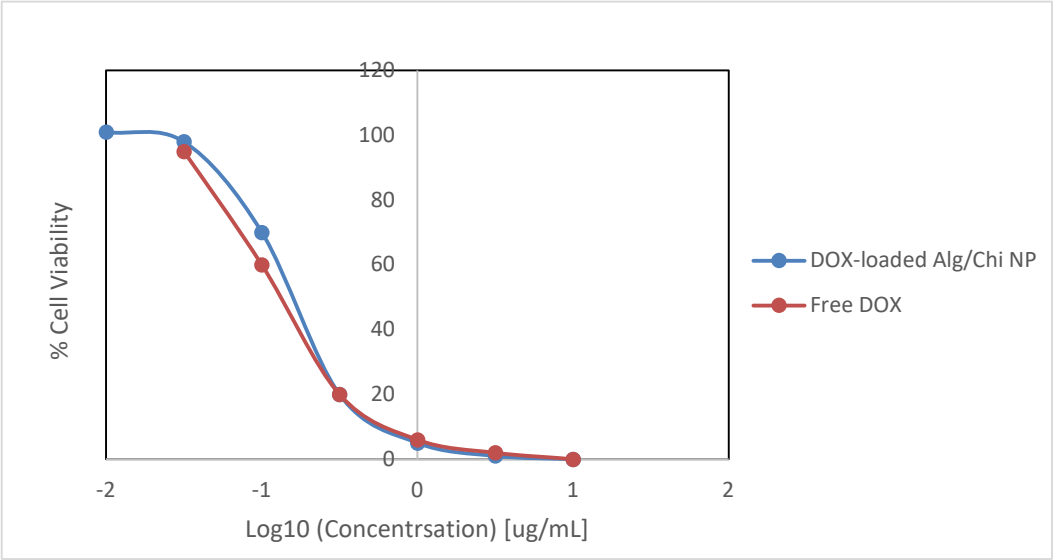

(a)

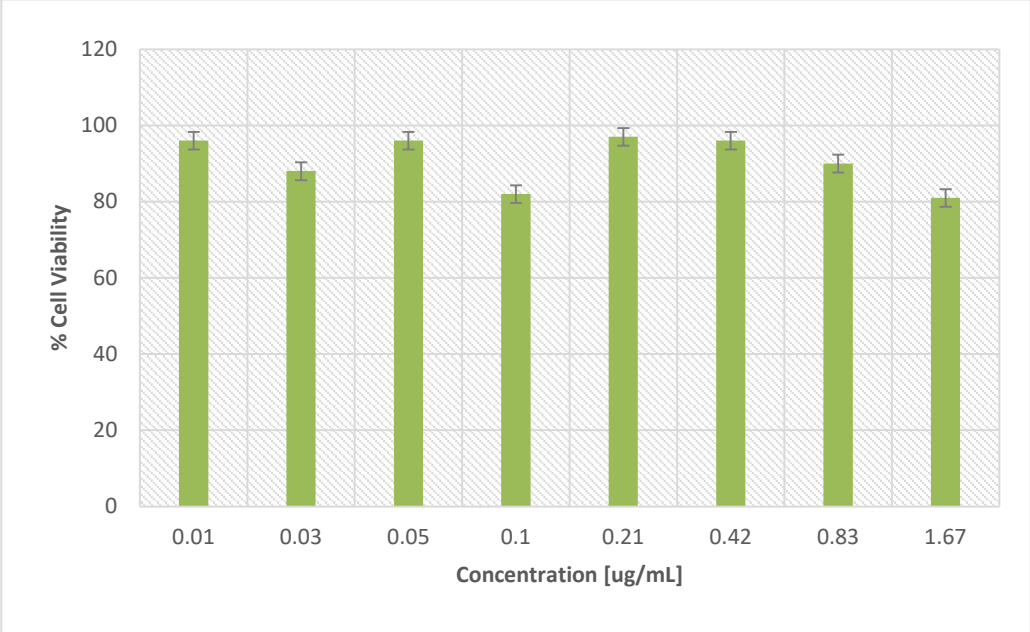

(b)

Fig. 7. Dose-response of 4 T1 cells to various treatments. (a) Cell viability after 72 h exposure to free/loaded DOX shows similar dose-response. (b) Cell viability after 72 h exposure to empty alginate-chitosan nanoparticles shows minimal toxicity associated with the drug carrier.

Conclusion

In conclusion, our experiment efficiently loaded doxorubicin into various sized chitosan/alginate for in vitro targeted administration applications on 4T1 breast cancer cells. Doxorubicin-loaded nanoparticles' ideal

loading efficiency, stability, and release profiles were identified. Following a 72-hour treatment period, cell viability was determined, and the IC50 values for free and encapsulated DOX were 0.13 and 0.15 µg/mL, respectively. While the nanoparticles are quite stable at pH 7.4, the alginate/chitosan NPs discharged the majority of the doxorubicin at pH 5.5. Chitosan/alginate NPs loaded with doxorubicin were taken up by the cells and aggregated around the nucleus, allowing the medication to be effectively administered close to the nucleus, where it exhibits its anti-cancer action, according to fluorescence microscopy pictures. For doxorubicin-resistant murin 4T1 breast cancer cells, chitosan/alginate nanoparticles loaded with the medication exhibited more toxicity than the free drug. This attests to the medication's potency after discharge. These findings suggest that the produced chitosan/alginate coated nanoparticles have a great deal of promise for application as a pH-responsive drug delivery system that may target tumor cells.

References

1. Ding J, Guo Y. Recent advances in chitosan and its derivatives in cancer treatment. Frontiers in Pharmacology. 2022 Apr 28;13:888740.
2. Persano F, Gigli G, Leporatti S. Lipid-polymer hybrid nanoparticles in cancer therapy: Current overview and future directions. Nano Express. 2021 Mar 18;2(1):012006.
3. Martinelli C, Biglietti M. Nanotechnological approaches for counteracting multidrug resistance in cancer. Cancer Drug Resistance. 2020;3(4):1003.
4. Fathi M, Abdolahinia ED, Barar J, Omidi Y. Smart stimuli-responsive biopolymeric nanomedicines for targeted therapy of solid tumors. Nanomedicine. 2020 Sep;15(22):2171-200.
5. Neerooa BN, Ooi LT, Shameli K, Dahlan NA, Islam JM, Pushpamalar J, Teow SY. Development of polymer-assisted nanoparticles and nanogels for cancer therapy: An update. Gels. 2021 May 17;7(2):60.
6. Eltayeb MA, Faggad A, Abbadi OS, Elhassan MM. Characteristics of Breast Cancer at First Presentation in Sudanese Patients Attending the National Cancer Institute–University of Gezira (NCI–UG). Archives of Breast Cancer. 2020 Aug 31:104-10.
7. Schroeder A, Heller DA, Winslow MM, Dahlman JE, Pratt GW, Langer R, Jacks T, Anderson DG. Treating metastatic cancer with nanotechnology. Nature Reviews Cancer. 2012 Jan;12(1):39-50.
8. Ferrari M. Nanovector therapeutics. Current opinion in chemical biology. 2005 Aug 1;9(4):343-6.
9. Wong KH, Lu A, Chen X, Yang Z. Natural ingredient-based polymeric nanoparticles for cancer treatment. Molecules. 2020 Aug 9;25(16):3620.
10. Shadabfar M, Abdouss M, Khonakdar HA. Synthesis, characterization, and evaluation of a magnetic molecular imprinted polymer for 5-fluorouracil as an intelligent drug delivery system for breast cancer treatment. Journal of Materials Science. 2020 Sep;55:12287-304.
11. Herdiana Y, Wathoni N, Gozali D, Shamsuddin S, Muchtaridi M. Chitosan-Based Nano-Smart Drug Delivery System in Breast Cancer Therapy. Pharmaceutics. 2023 Mar 8;15(3):879.
12. Avramović N, Mandić B, Savić-Radojević A, Simić T. Polymeric nanocarriers of drug delivery systems in cancer therapy. Pharmaceutics. 2020 Apr;12(4):298.
13. Neerooa BN, Ooi LT, Shameli K, Dahlan NA, Islam JM, Pushpamalar J, Teow SY. Development of polymer-assisted nanoparticles and nanogels for cancer therapy: An update. Gels. 2021 May 17;7(2):60.
14. Yang H, Hua S, Wang W, Wang A. Composite hydrogel beads based on chitosan and laponite: preparation, swelling, and drug release behaviour.
15. Dong Z, Wang Q, Du Y. Alginate/gelatin blend films and their properties for drug controlled release. Journal of Membrane Science. 2006 Sep 1;280(1-2):37-44.

16. Finotelli PV, Morales MA, Rocha-Leão MH, Baggio-Saitovitch EM, Rossi AM. Magnetic studies of iron (III) nanoparticles in alginate polymer for drug delivery applications. Materials Science and Engineering: C. 2004 Nov 1;24(5):625-9.
17. Du Y, Luo XL, Xu JJ, Chen HY. A simple method to fabricate a chitosan-gold nanoparticles film and its application in glucose biosensor. Bioelectrochemistry. 2007 May 1;70(2):342-7.
18. Kafshgari MH, Khorram M, Khodadoost M, Khavari S. Reinforcement of chitosan nanoparticles obtained by an ionic cross-linking process. Iran Polym J. 2011 May 1;20(5):445-56.
19. Murakami K, Aoki H, Nakamura S, Nakamura SI, Takikawa M, Hanzawa M, Kishimoto S, Hattori H, Tanaka Y, Kiyosawa T, Sato Y. Hydrogel blends of chitin/chitosan, fucoidan and alginate as healing-impaired wound dressings. Biomaterials. 2010 Jan 1;31(1):83-90.
20. Van der Lubben IM, Verhoef JC, Borchard G, Junginger HE. Chitosan for mucosal vaccination. Advanced drug delivery reviews. 2001 Nov 5;52(2):139-44.
21. Zohuriaan-Mehr MJ. Advances in chitin and chitosan modification through graft copolymerization: a comprehensive review. Iran Polym J. 2005 Mar 1;14(3):235-65.
22. Qi L, Xu Z, Jiang X, Hu C, Zou X. Preparation and antibacterial activity of chitosan nanoparticles. Carbohydrate research. 2004 Nov 15;339(16):2693-700.
23. Kutscher M, Cheow WS, Werner V, Lorenz U, Ohlsen K, Meinel L, Hadinoto K, Germershaus O. Influence of salt type and ionic strength on self-assembly of dextran sulfate-ciprofloxacin nanoplexes. International journal of pharmaceutics. 2015 May 30;486(1-2):21-9.
24. Chen YC, Hsieh WY, Lee WF, Zeng DT. Effects of surface modification of PLGA-PEG-PLGA nanoparticles on loperamide delivery efficiency across the blood–brain barrier. Journal of biomaterials applications. 2013 Mar;27(7):909-22.
25. Lertsutthiwong P, Noomun K, Jongaroonngamsang N, Rojsitthisak P, Nimmannit U. Preparation of alginate nanocapsules containing turmeric oil. Carbohydrate polymers. 2008 Oct 16;74(2):209-14.
26. Zhou J, Romero G, Rojas E, Ma L, Moya S, Gao C. Layer by layer chitosan/alginate coatings on poly (lactide-co-glycolide) nanoparticles for antifouling protection and Folic acid binding to achieve selective cell targeting. Journal of Colloid and Interface Science. 2010 May 15;345(2):241-7.
27. Motwani SK, Chopra S, Talegaonkar S, Kohli K, Ahmad FJ, Khar RK. Chitosan–sodium alginate nanoparticles as submicroscopic reservoirs for ocular delivery: Formulation, optimisation and in vitro characterisation. European Journal of Pharmaceutics and Biopharmaceutics. 2008 Mar 1;68(3):513-25.
28. Brezaniova I, Trousil J, Cernochova Z, Kral V, Hruby M, Stepanek P, Slouf M. Self-assembled chitosan-alginate polyplex nanoparticles containing temoporfin. Colloid and Polymer Science. 2017 Aug;295:1259-70.
29. Sarmento B, Ferreira D, Veiga F, Ribeiro A. Characterization of insulin-loaded alginate nanoparticles produced by ionotropic pre-gelation through DSC and FTIR studies. Carbohydrate polymers. 2006 Oct 5;66(1):1-7.
30. Tai K, He X, Yuan X, Meng K, Gao Y, Yuan F. A comparison of physicochemical and functional properties of icaritin-loaded liposomes based on different surfactants. Colloids and Surfaces A: Physicochemical and Engineering Aspects. 2017 Apr 5;518:218-31.
31. Tao L, Jiang J, Gao Y, Wu C, Liu Y. Biodegradable alginate-chitosan hollow nanospheres for codelivery of doxorubicin and paclitaxel for the effect of human lung cancer A549 cells. BioMed research international. 2018 Jan 28;2018.
32. Gautier J, Allard-Vannier E, Munnier E, Soucé M, Chourpa I. Recent advances in theranostic nanocarriers of doxorubicin based on iron oxide and gold nanoparticles. Journal of Controlled Release. 2013 Jul 10;169(1-2):48-61.

33. Wang Y, Zhang X, Yu P, Li C. Glycopolymer micelles with reducible ionic cores for hepatocytes-targeting delivery of DOX. International journal of pharmaceutics. 2013 Jan 30;441(1-2):170-80.
34. Tacar O, Sriamornsak P, Dass CR. Doxorubicin: an update on anticancer molecular action, toxicity and novel drug delivery systems. Journal of pharmacy and pharmacology. 2013 Feb;65(2):157-70.
35. Huan M, Zhang B, Teng Z, Cui H, Wang J, Liu X, Xia H, Zhou S, Mei Q. In vitro and in vivo antitumor activity of a novel pH-activated polymeric drug delivery system for doxorubicin.
36. Longhi A, Ferrari S, Bacci G, Specchia S. Long-term follow-up of patients with doxorubicin-induced cardiac toxicity after chemotherapy for osteosarcoma. Anti-cancer drugs. 2007 Jul 1;18(6):737-44.
37. Granados-Principal S, El-Azem N, Pamplona R, Ramirez-Tortosa C, Pulido-Moran M, Vera-Ramirez L, Quiles JL, Sanchez-Rovira P, Naudí A, Portero-Otin M, Perez-Lopez P. Hydroxytyrosol ameliorates oxidative stress and mitochondrial dysfunction in doxorubicin-induced cardiotoxicity in rats with breast cancer. Biochemical pharmacology. 2014 Jul 1;90(1):25-33.
38. Hilmer SN, Cogger VC, Muller M, Le Couteur DG. The hepatic pharmacokinetics of doxorubicin and liposomal doxorubicin. Drug metabolism and disposition. 2004 Aug 1;32(8):794-9.
39. Ke XY, Ng VW, Gao SJ, Tong YW, Hedrick JL, Yang YY. Co-delivery of thioridazine and doxorubicin using polymeric micelles for targeting both cancer cells and cancer stem cells. Biomaterials. 2014 Jan 1;35(3):1096-108.
40. Yang X, Hong H, Grailer JJ, Rowland IJ, Javadi A, Hurley SA, Xiao Y, Yang Y, Zhang Y, Nickles RJ, Cai W. cRGD-functionalized, DOX-conjugated, and 64Cu-labeled superparamagnetic iron oxide nanoparticles for targeted anticancer drug delivery and PET/MR imaging. Biomaterials. 2011 Jun 1;32(17):4151-60.
41. Xiong H, Du S, Ni J, Zhou J, Yao J. Mitochondria and nuclei dual-targeted heterogeneous hydroxyapatite nanoparticles for enhancing therapeutic efficacy of doxorubicin. Biomaterials. 2016 Jul 1;94:70-83.
42. Pongjanyakul T, Rongthong T. Enhanced entrapment efficiency and modulated drug release of alginate beads loaded with drug–clay intercalated complexes as microreservoirs. Carbohydrate Polymers. 2010 Jun 11;81(2):409-19.
43. Yuan Q, Shah J, Hein SR, Misra RD. Controlled and extended drug release behavior of chitosan-based nanoparticle carrier. Acta biomaterialia. 2010 Mar 1;6(3):1140-8.
44. Kuboi R. Reverse Micelle Size Distribution and Mechanism of Protein Solubilization Into The Reverse Micelles. Kagaku Kogaku Ronbunshu. 1990;16:763-71.
45. Kiyoyama S, Shiomori K, Kawano Y, Yoshizawa H, Yoshida M, Hatate Y. Characteristics of nano-capsules prepared using reverse micellar system. Chemical Engineering Research and Design. 2005 Jul 1;83(7):861-5.
46. Bodnar M, Hartmann JF, Borbely J. Preparation and characterization of chitosan-based nanoparticles. Biomacromolecules. 2005 Sep 12;6(5):2521-7.
47. Mitra S, Gaur U, Ghosh PC, Maitra AN. Tumour targeted delivery of encapsulated dextran–doxorubicin conjugate using chitosan nanoparticles as carrier. Journal of controlled release. 2001 Jul 6;74(1-3):317-23.
48. de Moura MR, Aouada FA, Mattoso LH. Preparation of chitosan nanoparticles using methacrylic acid. Journal of colloid and interface science. 2008 May 15;321(2):477-83.
49. Jiang X, Chen L, Zhong W. A new linear potentiometric titration method for the determination of deacetylation degree of chitosan. Carbohydrate Polymers. 2003 Dec 1;54(4):457-63.
50. Blanco E, Shen H, Ferrari M. Principles of nanoparticle design for overcoming biological barriers to drug delivery. Nature biotechnology. 2015 Sep;33(9):941-51.
51. Hu YB, Dammer EB, Ren RJ, Wang G. The endosomal-lysosomal system: from acidification and cargo sorting to neurodegeneration. Translational neurodegeneration. 2015 Dec;4:1-0.

52. Du G, Lin H, Wang M, Zhang S, Wu X, Lu L, Ji L, Yu L. Quercetin greatly improved therapeutic index of doxorubicin against 4T1 breast cancer by its opposing effects on HIF-1α in tumor and normal cells. Cancer chemotherapy and pharmacology. 2010 Jan;65:277-87.
53. Dönmez Y, Gündüz U. Reversal of multidrug resistance by small interfering RNA (siRNA) in doxorubicin-resistant MCF-7 breast cancer cells. Biomedicine & pharmacotherapy. 2011 Mar 1;65(2):85-9.